



Coudert, Y., Novák, O., & Harrison, C. J. (2019). A KNOX-Cytokinin Regulatory Module Predates the Origin of Indeterminate Vascular Plants. *Current Biology*, 29(16), 2743-2750.e5.
<https://doi.org/10.1016/j.cub.2019.06.083>

Peer reviewed version

License (if available):
CC BY-NC-ND

Link to published version (if available):
[10.1016/j.cub.2019.06.083](https://doi.org/10.1016/j.cub.2019.06.083)

[Link to publication record in Explore Bristol Research](#)
PDF-document

This is the author accepted manuscript (AAM). The final published version (version of record) is available online via Elsevier at <https://www.sciencedirect.com/science/article/pii/S0960982219308437#!>. Please refer to any applicable terms of use of the publisher.

University of Bristol - Explore Bristol Research

General rights

This document is made available in accordance with publisher policies. Please cite only the published version using the reference above. Full terms of use are available:
<http://www.bristol.ac.uk/red/research-policy/pure/user-guides/ebr-terms/>



Harrison, C. J., Coudert, Y., & Novak, O. (Accepted/In press). A KNOX-cytokinin regulatory module predates the origin of indeterminate vascular plants. *Current Biology*.

Peer reviewed version

[Link to publication record in Explore Bristol Research](#)
PDF-document

University of Bristol - Explore Bristol Research

General rights

This document is made available in accordance with publisher policies. Please cite only the published version using the reference above. Full terms of use are available:
<http://www.bristol.ac.uk/pure/about/ebr-terms>

**A KNOX-cytokinin regulatory module predates the origin of
indeterminate vascular plants.**

Yoan Coudert^{1,2,3}, Ondřej Novák⁴ and C. Jill Harrison^{1,2*}.

¹Plant Sciences Department, University of Cambridge, Downing Street, Cambridge, CB2 3EA, UK.

²School of Biological Sciences, University of Bristol, 24 Tyndall Avenue, Bristol, BS8 1TQ, UK.

³Laboratoire Reproduction et Développement des Plantes, Université de Lyon, ENS de Lyon, UCB Lyon 1,
CNRS, INRA, F-69342, Lyon, France.

⁴Laboratory of Growth Regulators, Centre of the Region Haná for Biotechnological and Agricultural
Research, Faculty of Science of Palacký University and Institute of Experimental Botany CAS, Šlechtitelů 27,
78371 Olomouc, Czech Republic.

*Lead Author: jill.harrison@bristol.ac.uk

*Lead Contact: jill.harrison@bristol.ac.uk

Summary

The diverse forms of today's dominant vascular plant flora are generated by the sustained proliferative activity of sporophyte meristems at plants' shoot and root tips, a trait known as indeterminacy [1]. Bryophyte sister lineages to the vascular plants lack such indeterminate meristems and have an overall sporophyte form comprising a single small axis which ceases growth in the formation of a reproductive sporangium [1]. Genetic mechanisms regulating indeterminacy are well characterised in flowering plants, involving a feedback loop between Class I *KNOX* genes and cytokinin [2, 3], and Class I *KNOX* expression is a conserved feature of vascular plant meristems [4]. The transition from determinate growth to indeterminacy during evolution was a pre-requisite to vascular plant diversification, but mechanisms enabling the innovation of indeterminacy are unknown [5]. Here we show that Class I *KNOX* gene activity is necessary and sufficient for axis extension from an intercalary region of determinate moss shoots. As in *Arabidopsis*, Class I *KNOX* activity can promote cytokinin biosynthesis by an *ISOPENTENYL TRANSFERASE* gene, *PpIPT3*. *PpIPT3* promotes axis extension, and *PpIPT3* and exogenously applied cytokinin can partially compensate for loss of Class I *KNOX* function. By outgroup comparison, the results suggest that a pre-existing *KNOX*-cytokinin regulatory module was recruited into vascular plant shoot meristems during evolution to promote indeterminacy, thereby enabling the radiation of vascular plant shoot forms.

Results and discussion

MKN2 is necessary and sufficient to promote sporophyte axis extension in Physcomitrella

Previous reports have identified roles for an intercalary region in promoting moss sporophyte extension [6], and identified three Class I *KNOX* genes; *Moss KNOX 2 (MKN2)*, *MKN4* and *MKN5*. Whilst *mkn4* and *mkn5* mutants have mild developmental defects, *mkn2* mutants have defective setae, but the developmental basis of such defects was not clear [7, 8]. To interrogate necessity and sufficiency of Class I *KNOX* function for axial extension in determinate moss shoots, we first staged wild-type (WT) sporophyte development in *Physcomitrella* (Figure 1A, 1C) in comparison to the development of *mkn2* mutants (Figure 1B, 1C). Seven distinct stages were identified in WT sporophytes and were morphologically marked by (1) apical cell divisions, (2) apical cell and merophyte divisions, (3) merophyte divisions following cessation of apical cell activity, (4) proliferative activity in an intercalary region, (5) swelling sporangia, (6) the earliest visible stages of columella development and (7) full capsule expansion with a visible columella (Figure 1A, 1C). In *mkn2* mutant sporophytes, we were able to identify each aforementioned stage except stage 4, when there is normally intercalary extension (Figure 1B, 1C). To quantify differences between WT and *mkn2* mutant plants, we measured the seta-foot (SF) to sporophyte (SP) length ratio (Figure 1A, 1B, 1D). This analysis revealed a reduction in SF to SP length ratio from about 40% in WT sporophytes to 30% in mutants, supporting the notion that intercalary extension is impaired in *mkn2* mutants (Figure 1D). Thus, *MKN2* is necessary for correct sporophyte axis extension. To test whether *MKN2* is sufficient to promote intercalary extension, we expressed a full length *MKN2* cDNA under control of the maize ubiquitin promoter in WT

sporophytes using the *pTHUBI>>MKN2* vector (See STAR Methods and Figure S1). Whilst most *MKN2oe* transgenic plants obtained were sterile, the elongated setae of sporophytes obtained in two independent transgenic lines (n = 6) suggested that *MKN2* over-expression promotes axis extension (Figure 1E). To circumvent sterility problems, we introduced an *MKN2*-glucocorticoid receptor (GR) fusion into the *mkn2* mutant background under control of the maize ubiquitin promoter (Figure 1F-1I). This permitted constitutive expression of an *MKN2*-GR fusion protein and allowed *MKN2* relocation to the nucleus to activate downstream targets following dexamethasone application, and an *mkn2* mutant line was transformed with a *GR* expression cassette (*mkn2/GR*) as a negative control (Figure 1F-1I). Transgenic plants were grown in sporophyte inducing conditions (see STAR Methods), and following fertilization, one *mkn2/GR* and two *mkn2/MKN2-GR* transgenic lines were soaked in a mock or 1 μ M dexamethasone solution. Whilst no morphological effect of dexamethasone on the *mkn2/GR* control line was observed, dexamethasone application to *mkn2/MKN2-GR* transgenic lines resulted in the development of mature sporophytes in which the SF/SP length ratio increased by about 5-10% (Figure 1H-1I). Both gain of function approaches yielded data that were consistent with a role for *MKN2* in promoting axis extension from an intercalary region in *Physcomitrella* sporophytes.

MKN2 suppresses the chloronema to caulonema transition and promotes gametophore initiation

Mosses have biphasic life cycles in which the multicellular gametophyte is dominant and comprises filamentous protonemata and shoot-like structures (gametophores). The spread of gametophytes across a surface is determined by the activity of two filament types whose segregated functions are marked by switches in cell identity and morphology; chloronemata have short cells with many chloroplasts and transverse cross walls, and caulonemata have longer cells with fewer chloroplasts and oblique cross walls [9]. Whilst some authors have found *MKN2* expression to be undetectable in gametophytes [8], others have identified up-regulation of *MKN2* expression in caulonemata [10] or gametophores [11], but no loss-of-function mutant phenotypes have been reported. We were unable to detect *MKN2* expression by RT-PCR in wild-type gametophyte tissues and confirmed that *mkn2* mutants have normal morphology in gametophytes (Figure S1), but wished to identify any developmental effects of ectopic *MKN2* expression. We found that *MKN2oe* transgenic lines had abnormal gametophyte phenotypes whose severity positively correlated with *MKN2* expression levels (Figure 2A and 2B, Figure S1). The most striking was that plant spread was reduced to about 40% of the WT area (Figure 2A and 2C), and we reasoned that this reduction could reflect a defective chloronema to caulonema transition. To test this hypothesis, we dissected filaments comprising over 8 cells from plants and measured the length of the first sub-apical cell and the second proximal cell of side-branches comprising 3 or more cells (Figure 2B and 2E). This sampling strategy was chosen to ensure like-for-like comparison of cell types in protonemal tissues with considerable variation in overall appearance. In WT plants, cell length was greater in primary filaments than in side-branches, but in *MKN2oe* plants both cell types had the same length as cells in WT side branches (Figure

2B, 2E). Furthermore, all cells had transversely oriented division walls, consistent with chloronemal identity (Figure 2F-2H). These data suggest that ectopic *MKN2* expression in gametophytes suppresses the normal switch from chloronema to caulonema identity in protonemal tissues. We also noted that the density of gametophores per plant was elevated to about 150% of WT levels, and gametophores initiated from chloronema cells (Figure S1) in *MKN2oe* plants (Figure 2D), suggesting that ectopic *MKN2* expression promotes gametophore initiation.

Plants with elevated cytokinin levels phenocopy MKN2 over-expressors

In *Physcomitrella*, the switch from chloronema to caulonema identity and gametophore initiation are both hormonally regulated by cytokinin; whilst cytokinin suppresses caulonema formation, it promotes gametophore initiation [12, 13]. Although previously published work suggests that Class I *KNOX* genes do not regulate cytokinin biosynthesis in *Physcomitrella* [8], the phenotypes of *MKN2oe* lines suggested perturbations in cytokinin levels. To test the hypothesis that the mutant phenotypes of *MKN2oe* transgenic lines reflect elevated cytokinin levels, we first treated WT plants with a range of concentrations of the aromatic cytokinin 6-benzylaminopurine (BAP) (Figure S2). We found that WT plants treated with 10 nM BAP had similar phenotypes to *MKN2oe* transgenics. Plant spread was reduced, the length of caulonemata sub-apical cells was reduced, and gametophore density was increased with respect to untreated controls (Figure 2A-2E). To determine whether elevating endogenous cytokinin levels similarly affected development, we grew transgenics in which overexpression of the *Physcomitrella* *ISOPENTENYL TRANSFERASE-1* gene (*PpIPT1oe*) up-regulates cytokinin biosynthesis [14]. In comparison to WT, *PpIPT1oe* transgenic lines had reduced plant spread and increased gametophore density, and sub-apical and side branch cell lengths were similar to WT side branch cell lengths (Figure 2A-2E). In both *PpIPT1oe* transgenic lines and BAP-treated WT plants, most filament tip cells had transversely oriented division walls, suggesting that filaments had chloronema identity (Figure 2F-2H). Thus, upregulation of an endogenous cytokinin biosynthesis pathway can trigger similar developmental responses to exogenously applied cytokinin and *MKN2* over-expression in *Physcomitrella* gametophytes.

MKN2 promotes cytokinin biosynthesis via PpIPT3

To determine whether *MKN2* promotes cytokinin biosynthesis, we quantified cytokinin levels in three independent *MKN2oe* transgenic lines by liquid chromatography coupled to tandem mass spectrometry (LC-MS/MS) [14, 15] (Figure 3A). Twenty-five different cytokinin types were analysed: isopentenyladenine (iP), *trans*-zeatin (tZ), *cis*-zeatin (cZ) and dihydrozeatin (DHZ), and their nucleotide, nucleoside and glycoside derivatives. Eleven cytokinin types were detected, including the gametophore-inducing cytokinins iP, isopentenyladenosine (iPR) and tZ [16]. All cytokinins showed increased levels in *MKN2oe* transgenic lines relative to WT controls, except isopentenyladenosine-5'-monophosphate (iPR5'MP), *trans*-zeatin riboside *O*-glucoside (tZROG) and tZ that were slightly reduced in *MKN2oe#1* and *MKN2oe#3* plants respectively (Figure 3A). Thus, ectopic *MKN2* expression is sufficient to promote cytokinin biosynthesis. In *Arabidopsis*,

KNOX proteins promote cytokinin biosynthesis by upregulating *IPT* expression [2, 3]. To determine how MKN2 up-regulates cytokinin biosynthesis in *Physcomitrella*, we first grew previously described dexamethasone-inducible *mkn2/MKN2-GR* expression lines (Figure 1) on 1 μ m dexamethasone or a mock control (Figure 3B). Whilst no morphological effect of dexamethasone on an *mkn2/GR* control line was observed, two *mkn2/MKN2-GR* lines had reduced spread in comparison to mock-treated controls, consistent with the notion that *MKN2* promotes cytokinin biosynthesis (Figure 3B, 3C). To test the hypothesis that *MKN2* acts via *PpIPTs*, we first searched the *Physcomitrella* genome for *IPT* homologues, finding six previously identified genes, *PpIPT1-PpIPT6* [8]. Our sequence analysis showed *PpIPT2* to lack a key functional domain and it was therefore discluded from further analyses as a likely pseudogene. We also found two further homologues that we named *PpIPT7* and *PpIPT8* (Figure S3, Data S1). We next analysed *PpIPT* expression patterns by a preliminary RT-PCR in an *mkn2/GR* control line and two *mkn2/MKN2-GR* lines before and after dexamethasone application (Figure 3D). Whilst *PpIPT6*, *PpIPT7* and *PpIPT8* expression was undetectable, RT-PCR showed down-regulation of *PpIPT5* expression following dexamethasone application, and MKN2-dependent up-regulation of *PpIPT1*, *PpIPT3* and *PpIPT4* expression (Figure 3D). We used three biological replicates of qRT-PCR to verify *PpIPT1*, *PpIPT3* and *PpIPT4* activation by MKN2. We were unable to confirm MKN2 activation of *PpIPT1* and *PpIPT4* expression, but found that *PpIPT3* expression strongly increased in response to dexamethasone application and relative to a *PpUBI* reference gene (Figure 3E). *PpIPT3* expression levels positively correlated with the strength of the mutant phenotype in transgenic lines (Figure 3B-3E), and expression was induced by four hours following dexamethasone treatment, suggesting that *PpIPT3* could be an early target of MKN2 (Figure S3). *PpIPT3* expression was also elevated in *mkn2/MKN2-GR* sporophytes following dexamethasone application (Figure 3F). These data suggest a role for MKN2 in promoting *PpIPT3* expression and cytokinin biosynthesis in *Physcomitrella* gametophytes, and in promoting *PpIPT3* expression in sporophytes.

***PpIPT3* promotes axial extension in *Physcomitrella* sporophytes**

In *Arabidopsis*, shoot indeterminacy depends on expression of both Class I *KNOX* and *IPT* genes, and loss-of-function *knox* mutant phenotypes are rescued by upregulated *IPT* expression [2, 3]. The data in Figure 3 show that in *Physcomitrella*, MKN2 can activate cytokinin biosynthesis by *PpIPT3*, suggesting that a KNOX-cytokinin regulatory interaction is conserved between *Arabidopsis* and *Physcomitrella*. However, most of these experiments were undertaken in an ectopic context in gametophytes, so inferences about homologies in meristem function between mosses and vascular plants should be made with caution. To further explore roles for cytokinin biosynthesis in sporophyte axis extension, we first analysed *PpIPT* expression patterns using *Physcomitrella* eFP Browser data [17], showing that *PpIPT3* was expressed at a relevant stage of sporophyte development (Figure S3). To test the potential involvement of *PpIPT3* in sporophyte axis extension, we engineered *Ppip3* mutant lines using a CRISPR approach with three guide RNAs targeted to exon 1 or exon 3 of the *PpIPT3* locus (See STAR Methods). These were used in pairs to

generate lines with three independent genomic deletions (Figure 4A), and sequencing showed that *Ppipt3^{CR#1}* and *Ppipt3^{CR#2}* lines had deletions of 70 or 117 amino acid residues in the predicted PpIPT3 protein sequence, respectively (Figure 4B). In contrast, the *Ppipt3^{CR#3}* line had a frame shift mutation that introduced a premature stop codon at position 140 of the predicted PpIPT3 protein sequence (Figure 4B). The mutant phenotypes of these three lines were characterised in both life cycle stages. *Ppipt3* gametophytes had disrupted morphology relative to wild-type plants, showing an increase in plant spread (Figure 4C, 4D). This phenotype fits well with prior understanding of hormone functions in protonemata [9, 18], and suggests that mutants have a lower cytokinin level permissive to a stronger chloronema to caulonema transition than normal. Whilst *Ppipt3^{CR#1}* and *Ppipt3^{CR#2}* mutant sporophytes showed no obvious phenotypic differences from WT sporophytes, the *Ppipt3^{CR#3}* mutant had sporophytes with a SF/SP length ratio that was significantly lower than WT (Figure 4E, 4F). The stronger effect of the *Ppipt3^{CR#3}* lesion than *Ppipt3^{CR#1}* and *Ppipt3^{CR#2}* lesions is consistent with the predicted effects of different mutant alleles on PpIPT3 protein structure and the notion that *PpIPT3* promotes sporophyte axis extension (Figure 4E, 4F).

PpIPT3 and cytokinin can partially compensate for loss of MKN2 function in Physcomitrella sporophytes

To further explore the link between MKN2, cytokinin and seta elongation, we first attempted to restore axis extension in *mkn2* mutants by *PpIPT* overexpression. However, this experiment rendered plants sterile or near-sterile, so it was not possible to quantify sporophyte phenotypes (Figure S4). We then attempted to complement the *mkn2* mutant phenotype by targeting the *PpIPT3* coding sequence into the *MKN2* locus in *mkn2* mutants (Figure 4G), which were originally generated by targeted replacement of *MKN2* with a G418 resistance cassette [8]. To verify *PpIPT3* targeting, *mkn2/MKN2*>>*PpIPT3* lines were first grown on selective media containing G418 (Figure 4H), and sensitive lines were then genotyped to confirm insertion of the *PpIPT3* cDNA into the *MKN2* locus (Figure 4I). Phenotypic characterisation showed that two lines had elevated SF/SP length ratios relative to *mkn2* mutants, suggesting that *PpIPT3* can partially compensate for loss of *MKN2* function (Figure 4J-K). Finally, we considered whether exogenously applied cytokinin can compensate for *mkn2* mutant defects by growing WT and mutant plants in sporophyte inducing conditions and soaking them in cytokinin after fertilization (Figure 4L-M). This showed that BAP and iP could both partially restore axis extension to *mkn2* sporophytes. Thus *PpIPT3* is likely to act downstream of MKN2 to produce cytokinin and promote intercalary meristem function and seta elongation in *Physcomitrella*.

This work aimed to explore genetic mechanisms involved in the origin of vascular plant meristems and hence focused on a mechanism operating in sporophytes. Previously published work showing that *Physcomitrella* Class I *KNOX* genes do not act via conserved downstream pathways used tissue from WT and *mkn2/4/5* triple mutant sporophytes in RT-PCR with primers to amplify 6 *PpIPT* homologues [8]. In contrast, we have taken a gain of function approach, showing that overexpression of a Class I *KNOX* gene can upregulate cytokinin biosynthesis in *Physcomitrella*, and a complementation approach showing that *PpIPT3* and cytokinin can partially compensate for loss of *KNOX* function. Whilst differences in technical

approach are one possible reason to account for the discrepancy between our results and previous results, it is also possible that *MKN2* could act antagonistically with *MKN4* and *MKN5* to regulate cytokinin biosynthesis in *Physcomitrella* sporophytes, and therefore their effect would be cancelled out in the *mkn2/4/5* triple mutants. The activation of cytokinin biosynthesis by a Class I KNOX protein in *Physcomitrella* suggests that a KNOX-cytokinin regulatory module is conserved between vascular plants and mosses, and reveals a fundamental role of *KNOX* genes. By outgroup comparison, it follows that vascular plant KNOX-cytokinin-regulated meristem functions may have derived directly from a functional unit operating in their ancestors, predating the origin of indeterminate sporophyte growth. We therefore propose that there is genetic homology between the proliferative zones of vascular plant meristems and the intercalary region of moss setae. We speculate more broadly on the evolution of land plant meristems elsewhere [1, 5, 19].

Acknowledgements

We thank Pierre-Francois Perroud for giving us the *pTHUbiGate* plasmid, Mike Prigge and Mark Estelle for giving us the *pMP1575* plasmid and Magdalena Bezanilla at Dartmouth College for pENTR-PpU6P-sgRNA-L1R5, pENTR-PpU6P-sgRNA-L5L2 and pMH-Cas9-gate plasmids. We thank Mitsuyasu Hasebe for the *mkn2* mutant. We thank Michaela Mrvková for help with cytokinin analyses. Jill Harrison thanks the Gatsby Charitable Foundation (GAT2962) and the Royal Society (UF130563) for fellowships supporting her work, and BBSRC for a grant (BB/L02248/1) supporting this project. Yoan Coudert thanks the University of Lyon, the CNRS and the ATIP-Avenir Fellowship programme for ongoing support. Ondřej Novák thanks the Ministry of Education, Youth and Sport of the Czech Republic, National Program for Sustainability (grant. LO1204) and ERDF project "Plants as a tool for sustainable global development" (No. CZ.02.1.01/0.0/0.0/16_019/0000827).

Author contributions

Y.C. and C.J.H. designed the project and wrote the manuscript. Y.C. performed all the experiments except for the cytokinin analyses (O.N.).

Declaration of interests

The authors declare no competing financial interests.

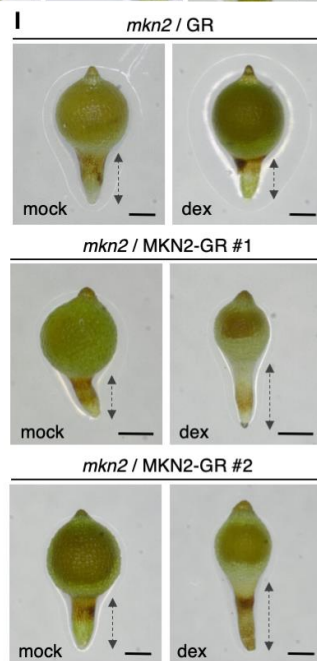
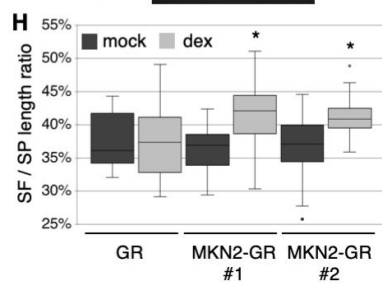
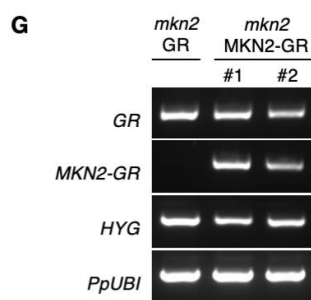
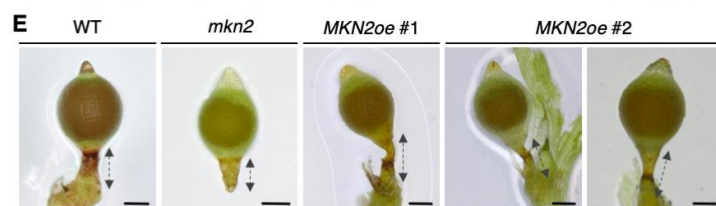
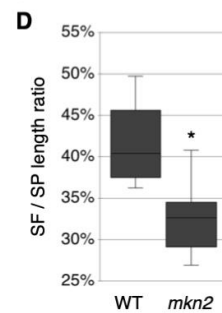
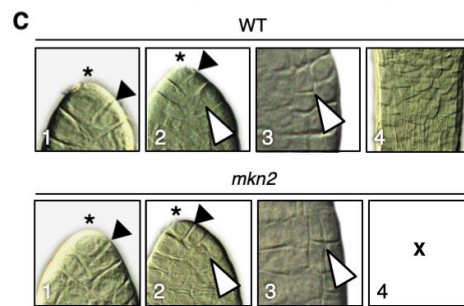
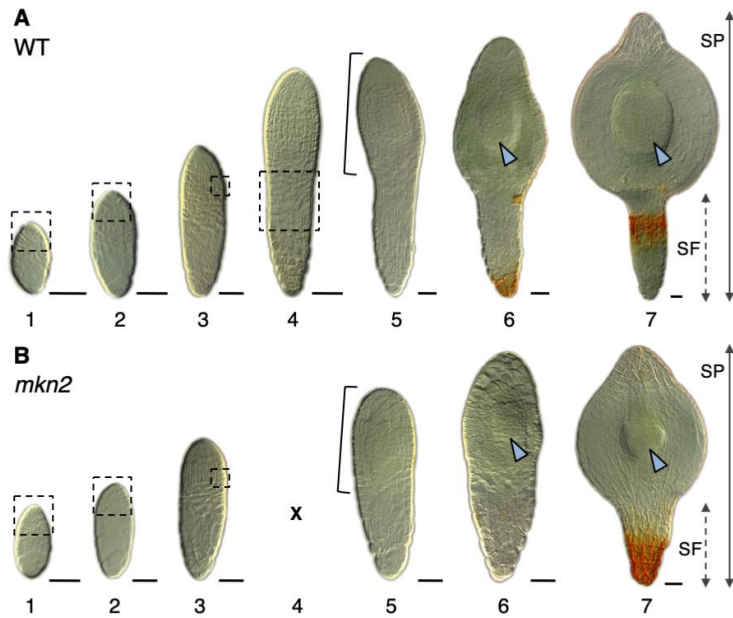


Figure 1. *MKN2* is necessary and sufficient for seta extension from an intercalary region in *Physcomitrella* sporophytes. Also see Figure S1.

(A, B) Differential interference contrast (DIC) micrographs of cleared wild-type ($n = 45$) (A) and *mkn2* ($n = 71$) (B) sporophytes. Stages are defined as follows: (1) apical cell divides, (2) apical cell and merophytes divide, (3) apical cell has stopped and merophytes divide, (4) intercalary meristem is active, (5) sporangium swells, (6) columella axis is visible and (7) columella axis is fully formed. Dashed boxes mark regions magnified in (C), brackets indicate swelling sporangia (5), blue arrowheads indicate columella axes (6, 7), and dashed and plain arrow lines indicate the seta-foot region (SF) and the full sporophyte length (SP), respectively. Scale bar = 50 μm . **(C)** Insets are close-ups of stages 1-4 and show apical cells (asterisks), apical cell and merophyte divisions (black and white arrowheads, respectively), and the intercalary region. **(D)** The seta-foot to sporophyte length ratio decreased significantly in *mkn2* mutants with respect to wild-type controls (Wilcoxon signed-rank test different from WT, $*p < 0.05$) ($n \geq 26$). **(E)** Mature sporophytes of *MKN2oe* transgenic lines showed elongated and bent seta relative to WT plants and *mkn2* mutants. **(F)** Schematic of the genetic construct, *pMP1575>>MKN2*, used to generate *MKN2-GR* over-expressing lines in the *mkn2* mutant background (*mkn2/MKN2-GR*). **(G)** PCR analysis detected the presence of glucocorticoid receptor gene (*GR*) and hygromycin selection marker (*HYG*) in all transgenic lines, and *MKN2-GR* transgene in *mkn2/MKN2-GR* lines only. *PpUBI* (Pp1s56_52_v6.1) was used as an internal control. **(H-I)** The seta-foot to sporophyte length ratio increased significantly in response to dexamethasone (dex) in *mkn2* lines over-expressing a *MKN2-GR* protein fusion, but not a *GR* protein only (Wilcoxon signed-rank test different from mock, $*p < 0.05$) ($n \geq 14$). Scale bar = 200 μm .

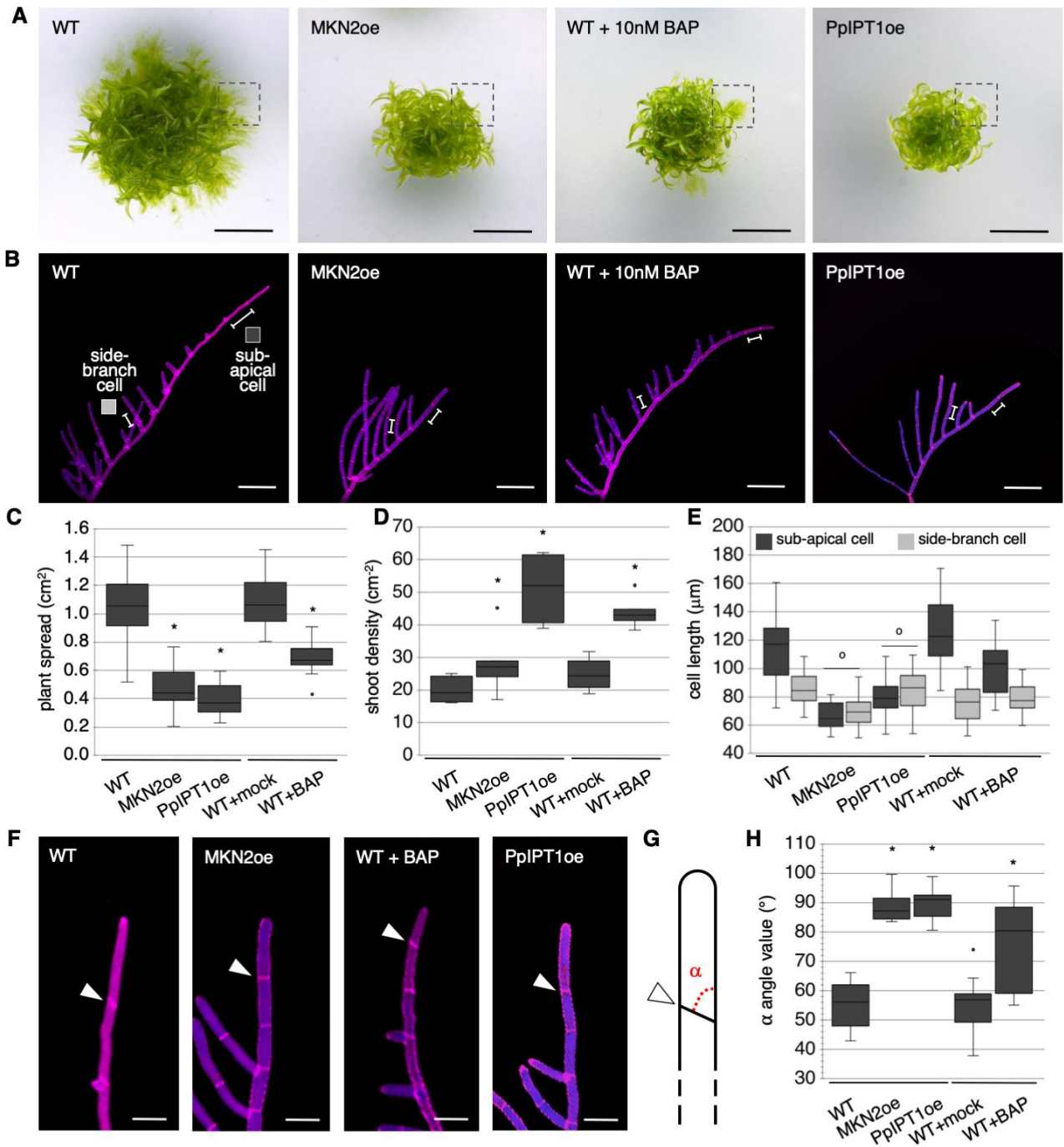


Figure 2. *MKN2* expression phenocopies cytokinin-mediated developmental change in *Physcomitrella* gametophytes. Also see Figure S2.

(A) Plant spread was reduced in *MKN2oe* and *PpIPT1oe* transgenics and plants treated with 10 nM 6-benzylaminopurine (BAP) relative to WT and mock-treated controls. Scale bar = 5 mm. **(B)** Confocal micrographs of Calcofluor stained protonemata showed that cells of the primary filaments were shorter in *MKN2oe*, *PpIPT1oe* and BAP-treated WT plants than in controls. Scale bar = 200 μ m. Boxes indicate cell types represented in (E). **(C-D)** Plant spread ($n \geq 16$) (C) and gametophore density ($n \geq 7$ colonies) (D) were significantly different from corresponding controls in *MKN2oe* and *PpIPT1oe* transgenics and BAP-treated WT plants (Wilcoxon signed-rank test different from control, * $p < 0.05$). **(E)** Sub-apical and side-branch cell

lengths ($n \geq 24$) were not significantly different from each other in *MKN2oe* and *PpIPT1oe* transgenics (Wilcoxon signed-rank test, $^{\circ}p > 0.05$), and were more similar to each other in BAP-treated WT plants than to corresponding controls. **(F)** Close-up of confocal microscope images shown in (B). White arrowheads indicate cell division planes at the tip of protonemal filaments. Scale bar = 60 μm . **(G)** Diagram of the tip of a protonemal filament. Arrowhead indicates division walls, and alpha (α) indicates the orientation of division plane with respect to the filament axis. **(H)** Alpha angle values of WT plants were close to 55° which corresponds to an oblique cell division plane and caulonemal identity. Alpha angle values of *MKN2oe* and *PpIPToe* plants were close to 90° indicating that cell division planes were transverse, showing chloronemal identity. Alpha angle values of BAP-treated WT plants were lower in average than *MKN2oe* and *PpIPToe* lines but significantly higher than mock-treated WT plants ($n = 15$; Wilcoxon signed-rank test different from control, $*p < 0.05$).

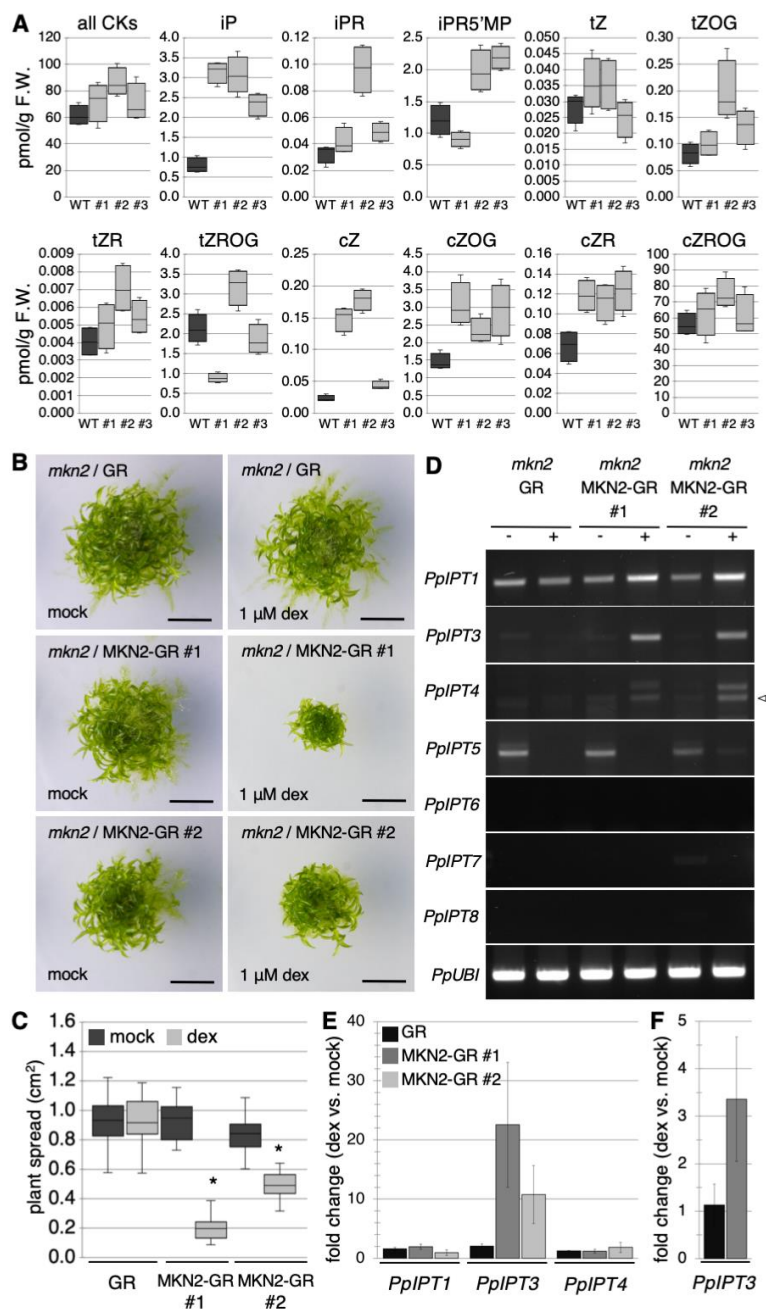


Figure 3. *MKN2* regulates cytokinin levels in *Physcomitrella* gametophytes, acting via *PpIPT3*. Also see Figure S3.

(A) Cytokinin (CK) profiling by LC-MS/MS showed a global increase in CK levels in three independent *MKN2oe* transgenic lines (#1, #2 and #3) relative to WT controls. *MKN2oe* #1 is the line shown in Figure 2 (see Figure S1 for *MKN2oe* #2 and #3 transgenic line phenotypes). Box plots represent data from four biological replicates and CK levels are expressed in pmol per gram of fresh weight (pmol/g F.W.). iP, isopentenyladenine; iPR, isopentenyladenosine; iPR5'MP, isopentenyladenosine-5'-monophosphate; tZ, *trans*-zeatin; tZR, *trans*-zeatin riboside; tZOG, *trans*-zeatin *O*-glucoside; tZROG, *trans*-zeatin riboside *O*-glucoside; cZ, *cis*-zeatin; cZR, *cis*-zeatin riboside; cZOG, *cis*-zeatin *O*-glucoside; cZROG, *cis*-zeatin riboside *O*-glucoside. **(B)** Plant spread was reduced in *mkn2/MKN2-GR* transgenics treated with 1 μ M dexamethasone (dex) relative to mock-treated controls, but remained similar in mock and dex-treated *mkn2/GR* transgenics. Scale bar = 5 mm. **(C)** Plant spread ($n \geq 14$) was significantly different in dex-treated *mkn2/MKN2-GR* transgenics and corresponding controls, but was similar in mock and dex-treated *mkn2/GR* transgenics (Wilcoxon signed-rank test, * $p < 0.05$). **(D)** RT-PCR analysis suggested probable induction of *PpIPT1*, *PpIPT3* and *PpIPT4* in response to 1 μ M dex in *mkn2/MKN2-GR* transgenics but not in *mkn2/GR* controls. Expression of *PpIPT5* and *PpIPT6-PpIPT8* was repressed by dex, or not detected respectively. *PpUBI* (Pp1s56_52_v6.1) was used as internal control. **(E)** Quantitative RT-PCR analysis showed that the expression of *PpIPT3* but not *PpIPT1* and *PpIPT4* was induced in *mkn2/MKN2-GR* in response to 1 μ M dex application, but there was no induction in *mkn2/GR* transgenics (mean fold change of three independent biological replicates \pm SE). **(F)** Quantitative RT-PCR analysis showed that *PpIPT3* expression was induced in *mkn2/MKN2-GR* sporophytes in response to 1 μ M dex application, but there was no induction in *mkn2/GR* controls (mean fold change of four independent biological replicates \pm SE).

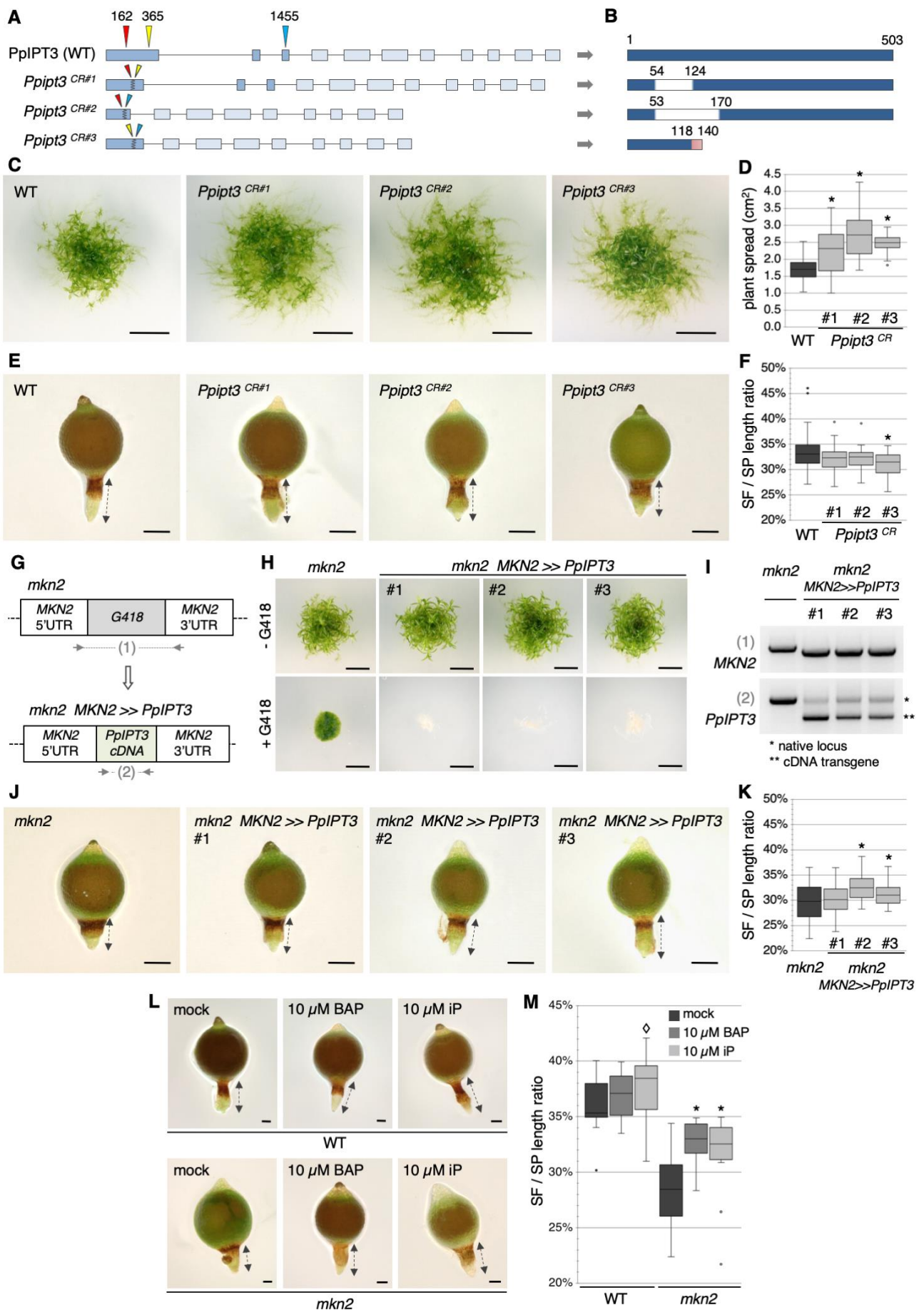


Figure 4. *PpIPT3* promotes sporophyte axis extension in wild-type plants and partially compensates for axis elongation defects in *mkn2* mutants. Also see Figure S3 and Figure S4.

(A) Architecture of the WT *PpIPT3* genomic locus showing the position of three *PpIPT3*-specific sgRNAs (arrowheads), and **(B)** resultant edits at the protein level revealed by sequencing. Blue boxes indicate WT sequence, white boxes indicate a deletion and a red box indicates a frame shift mutation. **(C)** Gametophyte spread was increased in *PpIPT3* mutants relative to WT controls (scale bar = 5 mm), and quantitative analysis **(D)** showed that gametophyte spread ($n \geq 26$) differed significantly (Wilcoxon signed-rank test different from control, $*p < 0.05$). **(E-F)** The seta-foot to sporophyte length ratio was significantly reduced in *PpIPT3*^{CR#3} sporophytes relative to WT controls (Wilcoxon signed-rank test different from mock, $*p < 0.05$) ($n \geq 34$). Scale bar = 250 μm . **(G)** Schematic showing the targeting strategy used to generate *mkn2* *MKN2*>>*PpIPT3* lines. **(H)** *mkn2* mutant gametophytes but not *mkn2* *MKN2*>>*PpIPT3* transgenics were resistant to G418. Scale bar = 5 mm. **(I)** PCR analysis detected the expected size shift at the *MKN2* locus after replacement of the G418 resistance cassette with the *PpIPT3* cDNA (1), and the presence of the *PpIPT3* cDNA in all *mkn2* *MKN2*>>*PpIPT3* transgenic lines but not the *mkn2* mutant (2). **(J-K)** The seta-foot to sporophyte length ratio was significantly increased in sporophytes of *mkn2* *MKN2*>>*PpIPT3* #2 and #3 transgenic lines in comparison to *mkn2* controls (Wilcoxon signed-rank test different from mock, $*p < 0.05$) ($n \geq 36$). Scale bar = 250 μm . **(L-M)** The seta-foot to sporophyte length ratio slightly increased in response to 10 μM iP or 10 μM BAP application in WT plants (Wilcoxon signed-rank test different from mock, $\diamond p < 0.08$), but increased more strongly in *mkn2* mutants (Wilcoxon signed-rank test different from mock, $*p < 0.05$) than in mock-treated controls ($n \geq 8$). Dashed line indicates the seta-foot region. Scale bar = 100 μm .

STAR METHODS

LEAD CONTACT AND MATERIALS AVAILABILITY

Further information and requests for resources and reagents should be directed to and will be fulfilled by the Lead Contact, Jill Harrison (jill.harrison@bristol.ac.uk). Please note that the transfer of transgenic materials will be subject to MTA and any relevant import permits.

EXPERIMENTAL MODELS AND SUBJECT DETAILS

Physcomitrella plant growth

The Gransden strain of *Physcomitrella patens* was used as the wild-type background for generating *MKN2oe*, *mkn2*/GR, *mkn2*/MKN2-GR and *mkn2*/MKN2>>*PpIPT3* transgenic lines, and the Villersexel strain of *Physcomitrella patens* was used as the wild-type background for generating *PpIPT3* CRISPR mutants. Plants were cultivated in sterile conditions on BCDAT medium (250 mg/L MgSO₄·7H₂O, 250 mg/L KH₂PO₄

(pH 6.5), 1010 mg/L KNO₃, 12.5 mg/L, FeSO₄·7H₂O, 0.001% Trace Element Solution (0.614 mg/L H₃BO₃, 0.055 mg/L AlK(SO₄)₂·12H₂O, 0.055 mg/L CuSO₄·5H₂O, 0.028 mg/L KBr, 0.028 mg/L LiCl, 0.389 mg/L MnCl₂·4H₂O, 0.055 mg/L CoCl₂·6H₂O, 0.055 mg/L ZnSO₄·7H₂O, 0.028 mg/L KI and 0.028 mg/L SnCl₂·2H₂O), 0.92 g/L di-ammonium tartrate (C₄H₁₂N₂O₆) and 8 g/L agar with CaCl₂ added to a 1 mM concentration after autoclaving) at 23 °C in continuous light or under a 16h light/8h dark cycle, at 50-150 μmol^{m⁻²s⁻¹} in Panasonic MLR-351/352 growth cabinets. Phenotypic analyses of gametophyte development were undertaken using 1 mm² spot cultures. Sporophyte cultures were initiated from macerated protonemal cultures grown for 5-10 days on BCDAT plates overlain with cellophane discs and then transferred to rehydrated Jiffy-7 peat pellets. Sporophyte cultures were grown at 23°C in continuous light for 6-8 weeks, and transferred to 16°C in short day (8h photoperiod) and low light (40 μmol^{m⁻²s⁻¹}) conditions for a minimum of 3 weeks before collecting developing or mature sporophytes. For pharmacological treatments, 6-benzylaminopurine (BAP), isopentenyladenine (iP), dexamethasone (dex), cycloheximide (chx) or solvent controls (water for BAP and iP, 70% ethanol for dex and chx) were incorporated into BCDAT plates or used in water solutions to soak sporophyte cultures, at concentrations stated in the main text.

METHOD DETAILS

***PpIPT* identification and phylogenetic analysis**

Arabidopsis thaliana, *Oryza sativa* and *Selaginella moellendorffii* sequences were identified from [21] and [22], and *Physcomitrella* sequences were obtained by BLAST against the genome (accessible at Phytozome). All retrieved sequences were scanned against the InterPro protein signature databases to identify characteristic conserved domains. All *Physcomitrella* IPT (*PpIPT*) sequences except *PpIPT2* contained a dimethylallyltransferase domain (IPR039657) (see Data S1). *PpIPT2* was therefore considered a likely pseudo-gene and was excluded from phylogenetic analyses. Protein sequences were aligned using the multiple sequence alignment clustal omega tool (default parameters) and the tree was generated using the ClustalW2 phylogeny tool (default parameters). Figtree software was used for tree visualization. *Physcomitrella patens* gene identifiers are *PpIPT1*: Pp1s96_115V6.1, Pp3c3_37040V3.1; *PpIPT2*: Pp1s432_30V6.1; *PpIPT3*: Pp1s280_8V6.1, Pp3c27_70V3.1; *PpIPT4*: Pp1s64_135V6.1, Pp3c5_9400V3.1; *PpIPT5*: Pp1s14_391V6.1, Pp3c6_21360V3.1; *PpIPT6*: Pp1s341_1V6.1, Pp3c16_6080V3.1; *PpIPT7*: Pp1s137_3V6.1, Pp3c23_12330V3.1; and *PpIPT8*: Pp1s137_19V6.1, Pp3c23_12370V3.1.

Molecular biology

Genomic DNA extraction

To genotype mutants, around 100 mg of 1 to 2-week old protonemal tissues were ground in liquid nitrogen and resuspended in 700 μl of DNA extraction buffer (2 % Hexadecyltrimethylammonium bromide (CTAB), 1.42 M NaCl, 100 mM Tris-HCl pH 8, 20 mM EDTA pH 8, 2 % PVP and 40 μg/ml RNaseA). Samples were

incubated for 10 minutes at 65 °C and centrifugated at 15,000 g for 10 min. Supernatant was transferred to a clean microtube and vigorously mixed with 600 µl of 24:1 chloroform:isoamyl alcohol. Samples were centrifuged at 15,000 rcf for 10 min, the aqueous phase was transferred to a new tube and mixed with 450 µl of isopropanol to precipitate DNA. Following centrifugation at 15,000 rcf for 10 min, DNA was washed with 200 µl of 70 % ethanol, air-dried for 15 min and resuspended in 50 µl of 10 mM Tris pH 8.0 with 1 mM Na₂EDTA.

Genotyping

Transgenic lines were genotyped by PCR using standard Taq Polymerase (e.g. GoTaq Polymerase) and 1 µl of CTAB-extracted genomic DNA per PCR reaction. The melting temperature of all primers was between 58 and 60°C, and sequences are listed in Table S1. PCR amplification conditions were adapted to each amplicon according to the manufacturer's instructions. *MKN2oe* lines were screened using *MKN2* forward-1 and *MKN2* reverse-1 primers (*MKN2* cDNA). *mkn2/GR* and *mkn2/MKN2-GR* lines were screened using *HYG* forward and *HYG* reverse primers (*HYG* resistance cassette), and *GR* forward and *GR* reverse primers (*Glucocorticoid receptor* gene), and *MKN2-GR* forward and *MKN2-GR* reverse primers (*Glucocorticoid receptor – MKN2* fusion gene). *Ppipt3 CR#1* mutants were screened using *Ppipt3-23F* and *Ppipt3-26R* primers, and *Ppipt3 CR#2* and *CR#3* mutants were screened using *Ppipt3-23F* and *Ppipt3-23R* primers. *mkn2 MKN2 >>PpIPT3* lines were screened using *IPT3-14F* and *IPT3-14R* primers (*PpIPT3* cDNA transgene) and *MKN2locus-3F* and *MKN2locus-3R* primers (*MKN2* locus). Integration of the full length *PpIPT3* cDNA into the *MKN2* locus was further confirmed by amplifying and sequencing *MKN2/PpIPT3* cDNA borders using *MKN2-5'UTR-24F* and *IPT3-5'-24R*, and *IPT3-3'-25F* and *MKN2-3'UTR-25R* primer pairs, respectively. *PpUBI* was used as a positive control and detected using *PpUBI* forward-1 and *PpUBI* reverse-1 primers.

RT-PCR

Total RNA was isolated from 7 or 28-day old spot cultures using the QIAGEN RNeasy™ method. RNA was DNase treated prior to reverse transcription with SuperScript® II following manufacturer's guidelines. Semi-quantitative RT-PCR was undertaken using *UBIQUITIN* (Pp1s56_52V6.1) as a loading control, which was amplified using *PpUBI* forward-2 and *PpUBI* reverse-2, or *PpUBI* forward-3 and *PpUBI* reverse-3 primers. *PpIPT1*, *PpIPT3-PpIPT8* and *MKN2* genes were respectively amplified using the following primer pairs: *PpIPT1* forward and *PpIPT1* reverse, *PpIPT3* forward and *PpIPT3* reverse, *PpIPT4* forward and *PpIPT4* reverse, *PpIPT5* forward and *PpIPT5* reverse, *PpIPT6* forward and *PpIPT6* reverse, *PpIPT7* forward and *PpIPT7* reverse, *PpIPT8* forward and *PpIPT8* reverse, and *MKN2* forward-4 and *MKN2* reverse-4. Primer melting temperatures were between 58 and 60°C. PCR amplification conditions were 94°C 3 min; 94°C 30 sec, 58°C 30 sec, 72°C 45 sec (36 cycles); 72°C 5 min.

Quantitative RT-PCR

For gametophyte expression analyses, RNA and cDNA were prepared as described above. For sporophyte expression analyses, total RNA was isolated from immature sporophytes using the APPLIED BIOSYSTEMS Arcturus PicoPure RNA isolation kit (Cell Pellets protocol) following manufacturer's guidelines. qRT-PCR was performed using a Brilliant III UltraFast SYBR green master mix and a Stratagene Mx3005P bioanalyser, or a ROCHE Fast Start Universal SYBR Green master mix and a ThermoFisher StepOnePlus Real-Time PCR System. Thermocycling conditions were: 95°C 3 min; 95°C 5 sec, 60°C 20 sec (40 cycles). For sporophyte cDNA only, a 10-cycle pre-amplification PCR was performed prior to qRT-PCR analysis. Specificity of PCR amplification was checked by melt curve analysis at each run. *PpIPT1*, *PpIPT3*, *PpIPT4* and *PpUBI* genes were respectively amplified using the following primer pairs: *PpIPT1* forward-1 and *PpIPT1* reverse-1, *PpIPT3* forward-1 and *PpIPT3* reverse-1, *PpIPT4* forward-1 and *PpIPT4* reverse-1, *PpUBI* forward-4 and *PpUBI* reverse-4. Primer melting temperatures were comprised between 58 and 60°C. Expression of *PpUBI* was used as a reference to normalize gene expression levels between conditions, and Ct values were converted into relative expression values using the comparative Ct method [23].

Cloning

Generation of MKN2 and MKN2-GR overexpression constructs

To construct the pTHUBI-MKN2 expression vector and generate *MKN2oe* lines, a full length MKN2 cDNA was isolated by successive rounds of PCR using three pairs of nested primers (*MKN2* forward-3 and *MKN2* reverse-3, *MKN2* forward-2 and *MKN2* reverse-2, and *MKN2* forward-1 and *MKN2* reverse-1). *MKN2* cDNA was then amplified using MKN2-AttB-F and MKN2-AttB-R primers, cloned into the pDONR221 entry vector using the Gateway BP Clonase II enzyme, and then into the pTHUBI-Gateway destination vector using the Gateway LR Clonase II enzyme. To construct the pMP1575-MKN2 expression vector and generate *mkn2*/*MKN2-GR* lines, an *MKN2* cDNA minus the stop codon was PCR amplified using MKN2-AttB-F and MKN2-AttB-R-noStop primers, cloned into pDONR207 using the Gateway BP Clonase II enzyme and then into the pMP1575 vector (a gift from Mike Prigge and Mark Estelle) using the Gateway LR Clonase II enzyme. The empty pMP1575 vector was used to generate *mkn2*/GR control lines.

Generation of PpIPT3 CRISPR constructs

The CRISPR-cas9 vector system described hereafter is based on Gateway Technology. Vectors were adapted from [24] for use in *Physcomitrella* by Magdalena Bezanilla's laboratory. To generate *PpIPT3* knock-out constructs, a protospacer corresponding to each sgRNA targeting exon 1 (positions 162 and 365) and exon 3 (position 1455) was designed using CRISPOR software. Corresponding oligo pairs (sgR-IPT3-EX1-162-F and sgR-IPT3-EX1-162-R, sgR-IPT3-EX1-365-F and sgR-IPT3-EX1-365-R, and sgR-IPT3-EX3-1455-F and sgR-IPT3-EX3-1455-R) were annealed and inserted downstream of a U6 promoter, into the *BsaI* site of the pENTR-PpU6p-sgRNA-L1R5 or pENTR-PpU6p-sgRNA-L5L2 entry vectors (a gift from Magdalena Bezanilla). Then, they were transferred to the pMH-Cas9-gate destination vector that contains the Cas9 enzyme coding sequence and a hygromycin resistance cassette for transient antibiotic selection, using the Gateway LR

Clonase II enzyme. Resulting plasmids were named pMH-Cas9_sgR-IPT3-EX1-162_EX1-365, pMH-Cas9_sgR-IPT3-EX1-162_EX3-1455 and pMH-Cas9_sgR-IPT3-EX1-365_EX3-1455, respectively.

Generation of MKN2>>PpIPT3 complementation constructs

Two plasmids were made to replace the G418 resistance cassette from the *mkn2* mutant with the full-length *PpIPT3* cDNA. The first was used to disrupt the *G418* coding sequence and provide transient hygromycin resistance for plant selection. A protospacer corresponding to a *G418* specific sgRNA was designed using the CRISPOR software. Corresponding oligos (sgR-G418-YCL1-F and sgR-G418-YCL1-R) were annealed and inserted downstream of a U6 promoter, into the *BsaI* site of the pENTR-PpU6p-sgRNA-L1L2, and then into pMH-Cas9-gate as described above to obtain pMH-Cas9_sgR-G418. The second plasmid contains the gene replacement cassette. 5' and 3' *MKN2* flanking regions, and a full length *PpIPT3* cDNA, were PCR amplified with the Phusion DNA polymerase using MKN2-5'-164-F and MKN2-5'-164-R, MKN2-3'-167-F and MKN2-3'-167-R, and IPT3-168-F and IPT3-168-R primer pairs, respectively. An MKN2-5' fragment was subcloned into pGEM-T EASY and, an MKN2-3' fragment was inserted downstream of the MKN2 5' fragment using *SpeI* and *NdeI* restriction sites. The *PpIPT3* cDNA fragment was subsequently cloned into the *SpeI* site between MKN2 5' and 3' fragments to obtain pGEMT-MKN2_5'-IPT3-MKN2_3'. Both plasmids were used together in a transformation to generate complementation lines.

***Physcomitrella* genetic transformation**

Plasmid DNA was purified using the QIAGEN Plasmid Plus Midi system and diluted in water at a concentration of 1 µg/µL prior to transformation. For overexpression approaches only, plasmid DNA was also linearized using *SwaI* (pTHUBI-MKN2) or *SfiI* (pMP1575-MKN2) restriction enzymes and cleaned up using a NucleoSpin Gel and PCR Clean-up or similar kit. All steps below were performed in sterile conditions. Protonemal cultures used for genetic transformation were initiated from 5-10 day old tissues and grown for 5 days maximum on BCDAT plates overlain with autoclaved cellophane disks. Protonemal tissue was digested in a 1% driselase / 8% mannitol solution for 1 hour or so, at room temperature. The resulting suspension was filtered through a 100 µm nylon mesh, and cells were centrifuged at 90 g for 4 minutes and washed in an 8% mannitol solution three times. Protoplasts were resuspended in 8% mannitol at a concentration of 3.2×10^6 cell/ml. In a 13 ml tube, 150 µl of the protoplast suspension was gently mixed with 150 µl of 2xMaMg (61 g/L MgCl₂, mannitol 80 g/L, MES 2 g/L, pH 5.6), 15 µl DNA per construct and 300 µl PEG solution (23.6 g/L Ca(NO₃)₂·4H₂O, 4.76 g/L HEPES, 72.8 g/L mannitol, 400 g/L PEG6000, pH 7.5). The PEG-protoplast mixture was heat shocked at 45°C for 5 minutes, cooled down at 20°C for a further 10 minutes and progressively diluted over one hour with 8% mannitol to reach a final volume of 12 ml. The protoplast suspension was centrifuged at 90 g for 4 minutes, resuspended in BCDAT with 8% mannitol and 10 mM CaCl₂, and incubated overnight at 23°C in the dark. The next day, The protoplast suspension was centrifuged at 90 g for 4 minutes and resuspended in BCDAT with 8% mannitol, 10 mM CaCl₂ and 0.4% agar and plated onto BCDAT plates containing 8% mannitol, 10 mM CaCl₂ and 0.8% agar and overlain with sterile

cellophane disks, and incubated at 23°C in photoperiod conditions described above. After 5 days, cellophane disks were transferred to BCDAT plates supplemented with 20 mg/L Hygromycin B. After 7 days, cellophane disks were transferred to BCDAT medium without antibiotic. A second round of antibiotic selection was performed for transformations involving stable insertion of the antibiotic resistance cassette (i.e. *MKN2oe*, *mkn2/GR* and *mkn2/MKN2-GR* lines). For CRISPR approaches involving transient selection, only one round of antibiotic selection was performed. All lines were screened by PCR, RT-PCR and/or sequencing as described in the Molecular Biology section.

Phenotyping and imaging

To assess whole plant and sporophyte phenotypes, 4 week-old spot cultures and mature sporophytes were imaged using a Keyence VHX-1000E digital microscope with a 20-50 X or 50-200 X objective. Filaments were dissected from 10 day-old cultures, stained with 0.1 % Calcofluor (Fluorescent Brightener 28) or 50 mg/ml Propidium Iodide, and imaged using Leica (Wetzlar, Germany) TCS5 or SP8 confocal microscopes with HCX PL FLUOTAR 10x/0.30, HC FLUOTAR L 25x/0.95 or HCX APO L 40x/0.80 objectives. Laser excitation used a Diode 405 line, and emission was collected from a 420–460 nm band. Quantitative measurements were undertaken using ImageJ or Keyence software. Gametophore density was calculated as the number of gametophores on a plant divided by the area of the plant. The proportion of gametophores with sporophytes was calculated following hand dissection of c. 100 gametophores from a sporophyte induction culture. DIC micrographs of sporophytes cleared in Hoyer's medium (15 g gum arabic, 100 g chloral hydrate, 10 g glycerol for 25 ml distilled water) were taken using a Leica DMRXA microscope with an HCPL APO 10 X/0.40 objective.

Cytokinin quantification

To quantify cytokinin profiles, 50 mg of tissue was isolated from 10-day old cultures and snap frozen in liquid nitrogen. Samples were processed as described in detail in a methods paper published by Novák et al. (2008) [15].

QUANTIFICATION AND STATISTICAL ANALYSIS

Statistical analyses were undertaken using R. Experimental sample sizes and statistical methods detail are given in the legends for Figures 1-4 and S1-S4.

DATA AND CODE AVAILABILITY STATEMENT

IPT protein sequence data are included in Data S1. Further data are available on request from the lead author.

Data S1. IPT alignment used for phylogenetic analysis. Related to STAR Methods and Figure S3.

KEY RESOURCES TABLE

REAGENT or RESOURCE	SOURCE	IDENTIFIER
Bacterial and Virus Strains		
<i>E. coli</i> strain DH5 α	Widely distributed	N/A
<i>E. coli</i> strain DB3.1	Widely distributed	N/A
Chemicals and Recombinant Proteins		
GoTaq polymerase	Promega	Cat#M7122
Phusion High-Fidelity DNA polymerase	ThermoFisher	Cat#F530S
Superscript II reverse transcriptase	ThermoFisher	Cat#18064022
Restriction enzymes for cloning	New England Biolabs	N/A
DNase	Fermentas	Cat#EN0525
RNase A	ThermoFisher	Cat#R1253
Plant agar	Duchefa	Cat#P1001
Driselase (basidiomycetes sp.)	Sigma-Aldrich	Cat#8037
Polyethylene glycol (PEG) 6000	Sigma-Aldrich	Cat#81255
2-iP	Duchefa	Cat# D0906
6-Benzylaminopurine (6-BAP)	Duchefa	Cat# B0904
G418 disulphate	Melford	Cat#G0175
Hygromycin B	Melford	Cat#H7502
Dexamethasone	Sigma-Aldrich	Cat#D1756
Cycloheximide	Sigma-Aldrich	Cat#01810
Propidium iodide	Sigma-Aldrich	Cat#P4864
Calcofluor White / FB 28	Sigma-Aldrich	Cat#F3543
Chloral hydrate	Sigma-Aldrich	Cat#C8383
Gum arabic	Widely distributed	N/A
Glycerol	Widely distributed	N/A
Ethanol	Widely distributed	N/A
Chloroform	Widely distributed	N/A
Isoamyl alcohol	Widely distributed	N/A
D-mannitol	Sigma-Aldrich	Cat#M9647
MES	Sigma-Aldrich	Cat#69892
HEPES	Sigma-Aldrich	Cat#H3375
CTAB	Sigma-Aldrich	Cat#H6269
PVP	Sigma-Aldrich	Cat#PVP10
Critical Commercial Assays		
RNeasy RNA extraction kit	QIAGEN	Cat#74104

Plasmid Plus Midi kit	QIAGEN	Cat#12943
Arcturus PicoPure RNA Isolation Kit	ThermoFisher	Cat#KIT0204
Brilliant III UltraFast SYBR green master mix	Agilent	Cat#600882
Fast Start Universal SYBR Green master mix	Roche	Cat#04913914001
Gateway BP Clonase II enzyme mix	ThermoFisher	Cat#11789020
Gateway LR Clonase II enzyme mix	ThermoFisher	Cat#11791020
Nucleospin Gel and PCR Clean-up kit	Machery Nagel	Cat#740609.10
Experimental Models: Organisms/Strains		
<i>Physcomitrella patens</i> Gransden	Widely available	N/A
<i>Physcomitrella patens</i> Villersexel	Widely available	N/A
<i>Physcomitrella patens</i> <i>mkn2</i> mutant	[8]	N/A
<i>MKN2oe</i> #1 line	This study	N/A
<i>MKN2oe</i> #2 line	This study	N/A
<i>MKN2oe</i> #3 line	This study	N/A
<i>mkn2</i> / <i>GR</i> line	This study	N/A
<i>mkn2</i> / <i>MKN2-GR</i> #1 line	This study	N/A
<i>mkn2</i> / <i>MKN2-GR</i> #2 line	This study	N/A
<i>PpIPT3</i> CR#1 mutant	This study	N/A
<i>PpIPT3</i> CR#2 mutant	This study	N/A
<i>PpIPT3</i> CR#3 mutant	This study	N/A
<i>mkn2</i> <i>MKN2</i> >> <i>PpIPT3</i> #1 line	This study	N/A
<i>mkn2</i> <i>MKN2</i> >> <i>PpIPT3</i> #2 line	This study	N/A
<i>mkn2</i> <i>MKN2</i> >> <i>PpIPT3</i> #3 line	This study	N/A
Recombinant DNA		
pTHUBI-IPT1	[14]	N/A
pTHUBI-MKN2	This study	N/A
pMP1575-MKN2	This study	N/A
pGEMT-MKN2_5'-PpIPT3-MKN2_3'	This study	N/A
pMH-Cas9_sgR-G418	This study	N/A
pMH-Cas9_sgR-PpIPT3-EX1-162_EX1-365	This study	N/A
pMH-Cas9_sgR-PpIPT3-EX1-162_EX3-1455	This study	N/A
pMH-Cas9_sgR-IPT3-EX1-365_EX3-1455	This study	N/A
pENTR-PpU6p-sgRNA-L1R5	Bezanilla lab	Addgene 113737
pENTR-PpU6p-sgRNA-L5L2	Bezanilla lab	Addgene 113738
pENTR-PpU6p-sgRNA-L1L2	Bezanilla lab	Addgene 113735
pMH-Cas9-gate	Bezanilla lab	Addgene 113742
pMP1575	Estelle lab	N/A
pTHUBI-Gateway	[20]	N/A

pDONR221	ThermoFisher	Cat#12536017
pDONR207	Invitrogen	N/A
pGEMT-EASY	Promega	Cat#A1360
Software and Algorithms		
Clustal omega tool	www.ebi.ac.uk/Tools/msa	N/A
ClustalW2 phylogeny tool	www.ebi.ac.uk/Tools/phylogeny	N/A
Phytozome	www.phytozome.jgi.doe.gov/pz/portal.html	N/A
Figtree	www.tree.bio.ed.ac.uk/software/figtree	v1.4.3
CRISPR design software	www.crispor.tefor.net	N/A
ImageJ	www.imagej.net	v1.4.8
Addgene repository	www.addgene.org/kits/bezanilla-crispr-physcomitrella/	N/A
Moss eFP browser	www.bar.utoronto.ca/efp_physcomitrella/cgi-bin/efpWeb.cgi	N/A
Miscellaneous		
Jiffy-7 peat pellets (38 mm)	www.jiffypot.com/en/products/jiffy7.html	Widely distributed

References

- Harrison, C.J. (2017). Development and genetics in the evolution of land plant body plans. *Philosophical Transactions of the Royal Society B* 372, e20150490.
- Jasinski, S., Piazza, P., Craft, J., Hay, A., Woolley, L., Rieu, I., Phillips, A., Hedden, P., and Tsiantis, M. (2005). KNOX action in *Arabidopsis* is mediated by coordinate regulation of cytokinin and gibberellin activities. *Current Biology* 15, 1560-1565.
- Yanai, O., Shani, E., Dolezal, K., Tarkowski, P., Sablowski, R., Sandberg, G., Samach, A., and Ori, N. (2005). *Arabidopsis* KNOX1 proteins activate cytokinin biosynthesis. *Current Biology* 15, 1566-1571.
- Harrison, C.J., Corley, S.B., Moylan, E.C., Alexander, D.L., Scotland, R.W., and Langdale, J.A. (2005). Independent recruitment of a conserved developmental mechanism during leaf evolution. *Nature* 434, 509-514.
- Harrison, C.J., and Morris, J.L. (2017). The origin and early evolution of vascular plant shoots and leaves. *Philosophical Transactions of the Royal Society B* 373, e20160496.
- French, J., and Paolillo, D. (1975). Intercalary meristematic activity in the sporophyte of *Funaria* (Musci). *American Journal of Botany* 62, 86-96.
- Singer, S.D., and Ashton, N.W. (2007). Revelation of ancestral roles of *KNOX* genes by a functional analysis of *Physcomitrella* homologues. *Plant Cell Reports* 26, 2039-2054.

8. Sakakibara, K., Nishiyama, T., Deguchi, H., and Hasebe, M. (2008). Class 1 *KNOX* genes are not involved in shoot development in the moss *Physcomitrella patens* but do function in sporophyte development. *Evolution and Development* 10, 555-566.
9. Ashton, N.W., Grimsley, N.H., and Cove, D.J. (1979). Analysis of gametophytic development in the moss, *Physcomitrella patens*, using auxin and cytokinin resistant mutants. *Planta* 144, 427-435.
10. Horst, N.A., Katz, A., Pereman, I., Decker, E.L., Ohad, N., and Reski, R. (2016). A single homeobox gene triggers phase transition, embryogenesis and asexual reproduction. *Nature Plants* 2, 15209.
11. Frank, M.H., and Scanlon, M.J. (2015). Cell-specific transcriptomic analyses of three-dimensional shoot development in the moss *Physcomitrella patens*. *Plant Journal* 83, 743-751.
12. Cove, D.J., Schild, A., Ashton, N.W., and Hartmann, E. (1978). Genetic and physiological studies of the effect of light on the development of the moss, *Physcomitrella patens*. *Photochemistry and Photobiology* 27, 249-254.
13. Cove, D.J., Ashton, N.W., Featherstone, D.R., and Wang, T.L. (1979). The use of mutant strains in the study of hormone action and metabolism in the moss *Physcomitrella patens*. In Fourth John Innes Symposium. pp. 231-241.
14. Coudert, Y., Palubicki, W., Ljung, K., Novak, O., Leyser, O., and Harrison, C.J. (2015). Three ancient hormonal cues co-ordinate shoot branching in a moss. *eLIFE* 4, e06808.
15. Novák, O., Hauserová, E., Amakorová, P., Dolezal, K., and Strnad, M. (2008). Cytokinin profiling in plant tissues using ultra-performance liquid chromatography-electrospray tandem mass spectrometry. *Phytochemistry* 69, 2214-2224.
16. Von Schwatzenberg, Fernández Núñez, M.F., Blaschke, H., Dobrev, P.I., Novák, O., Motyka, V., and Strand, M. (2007). Cytokinins in the bryophyte *Physcomitrella patens*: analyses of activity, distribution, and cytokinin oxidase/dehydrogenase overexpression reveal the role of extracellular cytokinins. *Plant Physiology* 145, 786-800.
17. Ortiz-Ramirez, C., Hernandez-Coronado, M., Thamm, A., Catarino, B., Wang, M., Dolan, L., Feijo, J.A., and Becker, J.D. (2016). A transcriptome atlas of *Physcomitrella patens* provides insights into the evolution and development of land plants. *Molecular Plant* 9, 205-220.
18. Jang, G., and Dolan, L. (2011). Auxin promotes the transition from chloronema to caulonema in moss protonema by positively regulating *PpRSL1* and *PpRSL2* in *Physcomitrella patens*. *New Phytologist* 192, 319-327.
19. Harrison, C.J. (2015). Shooting through time: new insights from transcriptomic data. *Trends in Plant Science* 20, 468-470.

20. Perroud, P.-F., Cove, D.J., Quatrano, R.S., and McDaniel, S.F. (2011). An experimental method to facilitate the identification of hybrid sporophytes in the moss *Physcomitrella patens* using fluorescent tagged lines. *New Phytologist* 191, 301-306.
21. Yevdakova, N.A., and von Schwartzberg, K. (2007). Characterisation of a prokaryote-type tRNA-isopentenyltransferase gene from the moss *Physcomitrella patens*. *Planta* 226, 683-695.
22. Lindner, A.-C., Lang, D., Seifert, M., Podlešáková, K., Novák, O., Strnad, M., Reski, R., and von Schwartzberg, K. (2014). Isopentenyltransferase-1 (IPT1) knockout in *Physcomitrella* together with phylogenetic analyses of IPTs provide insights into evolution of plant cytokinin biosynthesis. *Journal of Experimental Botany* 65, 2533-2543.
23. Livak, K.J., and Schmittgen, T.D. (2001). Analysis of relative gene expression data using real-time quantitative PCR and the 2- $\Delta\Delta$ CT method. *methods* 25, 402-408.
24. Miao, J., Guo, D., Zhang, J., Huang, Q., Qin, G., Zhang, X., Wan, J., Gu, H., and Qu, L.-J. (2013). Targeted mutagenesis in rice using CRISPR-Cas system. *Cell Research* 23, 1233.

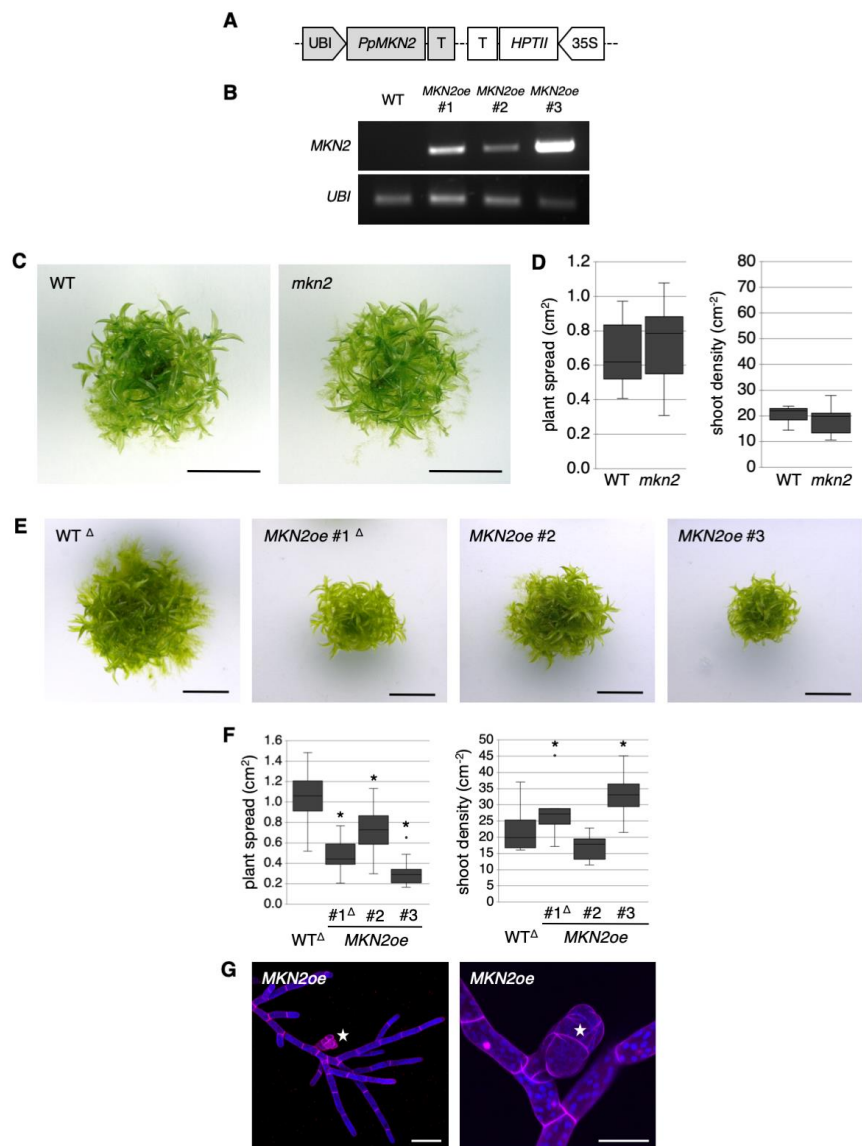


Figure S1. *MKN2* expression levels positively correlate with phenotype severity in *MKN2oe* lines. Related to Figure 1. (A) Schematic of the genetic construct (*pTHUBI*>>*MKN2*) used to generate *MKN2* over-expressing lines (*MKN2oe*). *35S* and *UBI*, constitutive promoters; *T*, Nos terminator; *HPTII*, hygromycin resistance gene. **(B)** RT-PCR analysis detected strong expression of *MKN2* in three independent *pTHUBI*>>*MKN2* (*MKN2oe*) transgenic lines but not in untransformed WT controls. *PpUBI* (Pp1s56_52_v6.1) was used as internal control. **(C)** Gametophytes appeared similar in WT and *mkn2* mutant plants. Scale bar = 5 mm. **(D)** Gametophyte spread ($n \geq 26$) and shoot density ($n \geq 10$ colonies) were similar (Wilcoxon signed-rank test $p > 0.05$) in WT and *mkn2* mutant plants. **(E)** Plant spread and protonemal elongation were reduced in proportion to *MKN2* expression levels in transgenic lines. *MKN2oe* #1 is shown in Figure 2. Scale bar = 5 mm. **(F)** Plant spread ($n \geq 21$) and shoot density ($n \geq 7$ colonies) were significantly different in different *MKN2oe* lines and WT plants (mean \pm SD; t-test different from WT, * $p < 0.05$). Triangles indicate data replicated from Figure 1. **(G)** Confocal micrographs of propidium iodide stained protonemata showed that gametophore buds (stars) initiated from chloronema cells in *MKN2oe* plants (blue, chlorophyll ; magenta, PI). Scale bar = 100 μ m.

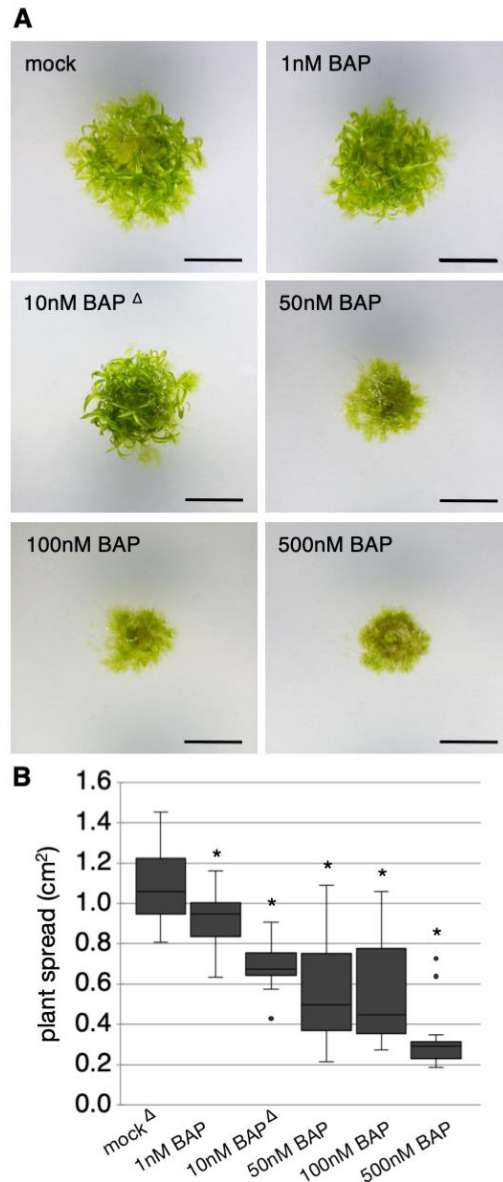


Figure S2. Exogenous cytokinin reduces protonemal elongation and colony area. Related to Figure 2. (A) WT plants treated with increasing concentrations of benzylaminopurine (BAP) showed proportional reduction in colony size and protonemal elongation. Gametophore development was impaired in plants treated with 50 nM BAP or more. Scale bar = 5 mm. **(B)** Colony area was significantly reduced in BAP treated plants compared to mock treated controls (mean \pm SD; n = 16; t-test different from mock, *p < 0.05). Triangles indicate data replicated from Figure 1.

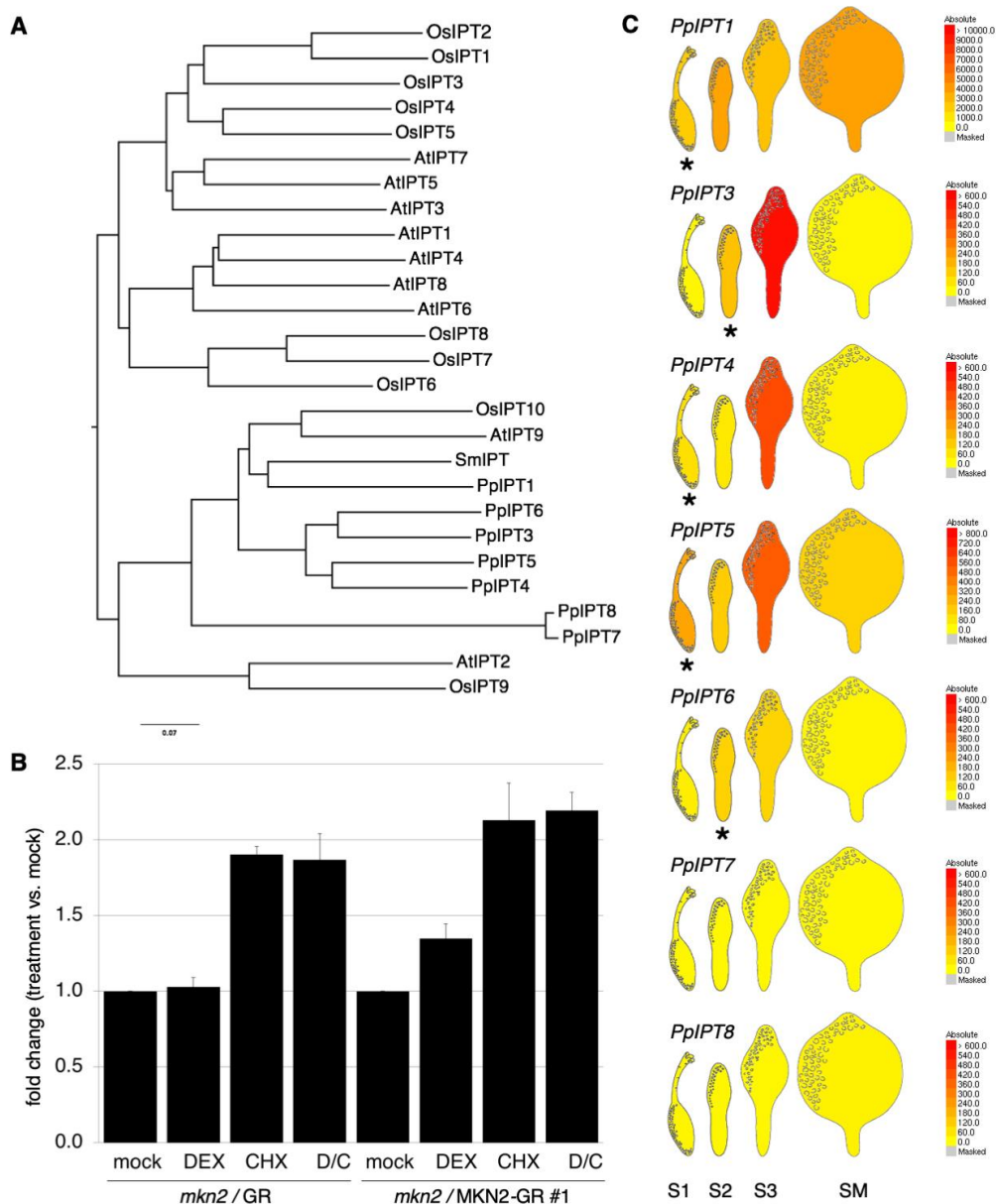


Figure S3. *PpIPTs* are active when the intercalary meristem is active. Related to Figure 3, Figure 4 and Data S1. (A) Relationship between IPT proteins from *A. thaliana*, *O. sativa*, *S. moellendorffii* and *P. patens*. The neighbour-joining tree was generated using the alignment of IPT amino acid sequences from *Arabidopsis thaliana*, *Oryza sativa*, *Selaginella moellendorffii* and *Physcomitrella patens* in Supplemental Dataset 1. **(B)** *PpIPT3* expression is induced by cyclohexamide (CHX) irrespective of the genetic background. Quantitative RT-PCR analysis of *PpIPT3* gene expression 4 hours after mock, 10 μ M dexamethasone (DEX), 10 μ M CHX or both 10 μ M DEX and 10 μ M CHX (D/C) treatment in *mkn2*/GR and *mkn2*/MKN2-GR #1 transgenic lines. *PpIPT3* gene expression is significantly induced by DEX in *mkn2*/MKN2-GR #1 plants and not *mkn2*/GR plants, but responds to CHX irrespective of the genetic background (mean fold change of two independent biological replicates relative to mock treatment \pm SE). **(C)** eFP Browser expression data for *Physcomitrella* IPT genes. Asterisks indicate stages at which expression was first detected, in the case of *PpIPT3* coinciding with intercalary meristem activity.

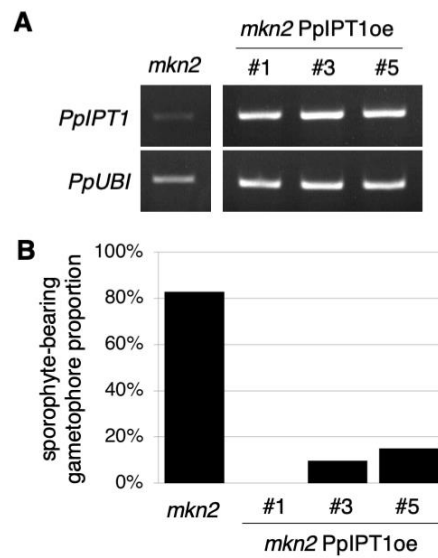


Figure S4. Effects of *PpIPT1* overexpression and exogenous cytokinin treatments on sporophyte development. Related to Figure 4. (A) RT-PCR analysis detected high levels of *PpIPT1* expression in gametophytes of different *mkn2 pTHUBI*>>*PpIPT1* (*PpIPT1oe*) lines in comparison to untransformed *mkn2* mutants. *PpUBI* was used as an internal control. **(B)** Bar plots show that the percentage of gametophores bearing at least one sporophyte was strongly or completely reduced relative to *mkn2* mutants in *mkn2/PpIPT1oe* transgenic lines (n ≥ 70 gametophores).

Table S1. Names and sequences of PCR primers used. Related to STAR Methods.

HYG forward
 HYG reverse
 GR forward
 GR reverse
 MKN2-GR forward
 MKN2-GR reverse
 PpUBI forward-1
 PpUBI reverse-1
 PpPT3-23F
 PpPT3-23R
 PpPT3-26R
 MKN2ocus-3F
 MKN2ocus-3R
 IPT3-14F
 IPT3-14R
 MKN2-5'UTR-24F
 IPT3-5'-24R
 IPT3-3'-25F
 MKN2-3'UTR-25R
 MKN2 forward-4
 MKN2 reverse-4
 PpUBI forward-2
 PpUBI reverse-2
 PpUBI forward-3
 PpUBI reverse-3
 PpIP71 forward
 PpIP71 reverse
 PpIP73 forward
 PpIP73 reverse
 PpIP74 forward
 PpIP74 reverse
 PpIP75 forward
 PpIP75 reverse
 PpIP76 forward
 PpIP76 reverse
 PpIP77 forward
 PpIP77 reverse
 PpIP78 forward
 PpIP78 reverse
 PpIP71 forward-1
 PpIP71 reverse-1
 PpIP73 forward-1
 PpIP73 reverse-1
 PpIP74 forward-1
 PpIP74 reverse-1
 PpUBI forward-4
 PpUBI reverse-4
 MKN2 forward-3
 MKN2 reverse-3
 MKN2 forward-2
 MKN2 reverse-2
 MKN2 forward-1
 MKN2 reverse-1
 MKN2-AttB-F
 MKN2-AttB-R
 MKN2-AttB-R-noStop
 sgR-G418-YCL1-F
 sgR-G418-YCL1-R
 sgR-IPT3-EX1-162-F
 sgR-IPT3-EX1-162-R
 sgR-IPT3-EX1-365-F
 sgR-IPT3-EX1-365-R
 sgR-IPT3-EX3-1455-F
 sgR-IPT3-EX3-1455-R
 MKN2-5'-164-F
 MKN2-5'-164-R
 MKN2-3'-167-F
 MKN2-3'-167-R
 IPT3-168-F
 IPT3-168-R

CGAAAAGTTCCGACAGCGTCT
 ACATTGTTGGAGCCGAAATC
 TTTTGACGATGGCTTTTCT
 TACCACAGCTCACCCTTACC
 TCACACTGGCCTTACCCTTC
 CCTTAGGAAGTGGAGAGAAAGC
 GCCATGCAGATCTTCGTGAA
 CTACGCAGCCAAAGAACCGA
 GTGGAGAATTAGTGGCGGGG
 TGCCAGTCGTTTCGAGCTAA
 AGCCGCTTAATTCATGAGC
 AATCCCGTCAAGSTGAGACAA
 TGCCGGTTTCTACGTTCCCTC
 GCGTCCCAATAGTTGAGGA
 TGCTTTTCCACAGGCTTCT
 TGGGTCGATCTTGTGACA
 ATTTACAGGCAGCAAGCTTC
 ACGGCGAGGTTATCCCTCT
 CAGCTGCCTTACAGTTGCT
 ATGGAGCAGCAAAACCC
 GAAGTATGATCAAACTTGG
 CCTGGCTGACTACAACATCC
 TGTCCGTCGAAATGGTTCCG
 TCCAGATCTTGTGAAGACC
 GCCCTCAAATGACAGAATCA
 AAGGCCACGAAGGAGGAT
 CACTTCAATGGCCCTTTCAT
 GCGTCCCAATAGTTGAGGA
 TGCTTTTCCACAGGCTTCT
 GACGCAGAAAGATCGTGTGA
 TACAGCTCCTTGGATGTTG
 TCAATGATGGAAATGCTGGA
 TGAGAAGCGTCAATCCAGTG
 GAGGGAATCCTGGAAACACA
 TGCGCTTATCAGAGCATTG
 GTGGAGCCGATGTATCTGT
 CTCCATGGCTTCTTCGTAGC
 CAATCGAGCTCGTAAACCC
 ACCAGACCCCTGGAGTTGTG
 CGATGGTACATGACTGGAAAG
 CCTCCACCTTCTTAATCAATC
 CCAGTTATCCCTCGAATTG
 CCTGTTCTTAGCCCTGTAGTG
 CCTAAGCAGCAACTACAC
 GCTCCTTGGATGTTGATAA
 AGTGGATGACTCCGGTAAG
 CAGTAGTGTGGTGGAAATG
 AATCCCGTCAAGSTGAGACAA
 ACGCGGCAGAATTTGGAA
 ACAAACTTCAAGTGGTGGACTTTG
 TTTATCTACATGGAGACTTCAAAAATG
 ATGGAGCAGCAAAACCC
 CTACTCCAGATGACCTCTGCA
 GGACAAGTTTGTACAAAAAGCAGGCTATGGAGCAGCAAAACCC
 GGACCACCTTGTACAAGAAAGCTGGGTCTACTCCAGATGACCTCTGCA
 GGACCACCTTGTACAAGAAAGCTGGGTCTCCAGATGACCTCTGCA
 CCATGTGTCCGGCTGTGAGCGCA
 AAAGTCCGCTGACAGCCGGAACAC
 CCATGTGCGCGCGAAAGTGGCTGT
 AAACACAGCCACTTTCGCGCGCAC
 CCATGTACGCGGTTGCGATGACT
 AAACAGTCTATCGCAACGCGTGAC
 CCATGGTTGATATTGTCCCTCCAA
 AAAGTGGAGGACAAATCAACC
 CAAATGCCAAAACGCTTTCT
 GAAACTATAGGGCTGGAAGGATG
 ACTAGTGAACAATCGAATCGTCTTCAGTG
 CATATGAAGCTCTAAATCCTTAATCTTGGAAAG
 ACTAGTATGTGGACTTCAAGAGCATGT
 ACTAGTTCAGAAATCTAACTAAATTTCTGTGAGC